PHYSICAL REVIEW A **76**, 012714 (2007)

Electron-impact ionization of diatomic molecules using a configuration-average distorted-wave method

M. S. Pindzola and F. Robicheaux
Department of Physics, Auburn University, Auburn, Alabama 36849, USA

J. Colgan
Theoretical Division, Los Alamos National Laboratory, Los Alamos, New Mexico 87545, USA

C. P. Ballance
Department of Physics, Rollins College, Winter Park, Florida 32789, USA

(Received 7 March 2007; published 19 July 2007)

Electron-impact ionization cross sections for diatomic molecules are calculated in a configuration-average distorted-wave method. Core bound orbitals for the molecular ion are calculated using a single-configuration self-consistent-field method based on a linear combination of Slater-type orbitals. The core bound orbitals are then transformed onto a two-dimensional (r,θ) numerical lattice from which a Hartree potential with local exchange is constructed. The single-particle Schrödinger equation is then solved for the valence bound orbital and continuum distorted-wave orbitals with S-matrix boundary conditions. Total cross section results for H_2 and N_2 are compared with those from semiempirical calculations and experimental measurements.

DOI: 10.1103/PhysRevA.76.012714 PACS number(s): 34.50.Gb

I. INTRODUCTION

Electron-impact ionization of diatomic molecules is an important collision process in many different areas of physics and chemistry. For example, electron ionization of H_2 and other first-row-element diatomic molecules is important in understanding divertor plasma dynamics in controlled fusion experiments [1]. In addition, the electron ionization of diatomic molecules is an example of the quantal three-body Coulomb breakup problem involving a nonspherical nuclear field. As such, it serves as a testing ground for the development of new theoretical methods to explain the increasingly detailed observations of the low-energy three-body breakup process [2].

Perturbative distorted-wave calculations of energy and angle differential cross sections for the electron ionization of diatomic molecules rely on accurate single-particle molecular continuum wave functions [3]. Nonperturbative R-matrix-with-pseudostates and time-dependent close-coupling calculations of total cross sections have been recently completed for the electron ionization of $H_2{}^+$ [4] and H_2 [5,6]. Extensions of the nonperturbative time-dependent close-coupling method to calculate energy and angle differential cross sections for the electron ionization of diatomic molecules will also rely on accurate molecular continuum wave functions as projection states.

As widely used for atomic targets, single-particle continuum wave functions may be obtained by expansion in spherical harmonics and numerical solution of the resulting one-dimensional (1D) radial Schrödinger equation. Although certainly viable for simple targets like H_2, such single-center spherical expansions for heavier molecules may become difficult to converge. Beginning with the pioneering work of Tully and Berry [7], single-particle continuum wave functions may also be obtained by expansion in rotational functions and numerical solution of the resulting 2D radial and angular Schrödinger equation [8,9].

Recently, we extended a configuration-average distorted-wave (CADW) method for atoms [10] to handle the calculation of electron-impact excitation and ionization cross sections for diatomic molecules [11]. The molecular CADW method relies on single-particle continuum wave functions obtained by solution of a 2D radial and angular Schrödinger equation. The CADW ionization cross sections for $H_2{}^+$ [11] were found to be in excellent agreement with previous distorted-wave calculations using single-particle continuum wave functions calculated in separable prolate spheroidal coordinates [12]. However, recent CADW ionization cross sections for H_2 [6] were found to be somewhat larger than expected, based on comparisons of CADW ionization cross sections with nonperturbative theory and experiment for He [13].

In this paper, we repeat our CADW calculations for the single ionization of H_2 using a modified version of the algorithm used to obtain single-particle continuum wave functions by solution of a 2D radial and angular Schrödinger equation. The key modification is the inclusion of the full S matrix in the numerical solution of the 2D radial and angular Schrödinger equation. This appears to completely eliminate all l mixing for neutral molecule scattering, no matter what the choice of box size. In addition, we make further CADW calculations for the single ionization of $N_2({}^1\Sigma_g^+)\rightarrow N_2{}^+({}^2\Sigma_g^+)$. In Sec. II we review the CADW cross section expressions and then present the new theory for the single-particle continuum wave functions. In Sec. III we present ionization cross sections for H_2 and N_2 and compare them with binary encounter Bethe calculations and experiment. In Sec. IV we give a brief summary. Unless otherwise stated, all quantities are given in atomic units.

II. THEORY

A. Distorted-wave ionization cross section

For atoms and diatomic molecules, the direct ionization cross section may be calculated using a configuration-average distorted-wave method [10,11]. The most general transition between configurations of a diatomic molecule is of the form

$$(nl\lambda)^w \epsilon_i l_i \lambda_i \rightarrow (nl\lambda)^{w-1} \epsilon_e l_e \lambda_e \epsilon_f l_f \lambda_f, \tag{1}$$

where w is the occupation number, and $nl\lambda$, $\epsilon_i l_i \lambda_i$, $\epsilon_e l_e \lambda_e$, and $\epsilon_f l_f \lambda_f$ are the quantum numbers of the bound valence electron and the incident, ejected, and final continuum electrons ($\lambda=|m|$ is the absolute value of the magnetic quantum number). The configuration-average ionization cross section is given by

$$\sigma_{ion} = \int_0^{E/2} d\epsilon_e \frac{64}{k_i^3 k_e k_f} \frac{w}{S(\lambda)} \sum_{l_i} \sum_{\lambda_i} \sum_{l_e} \sum_{\lambda_e} \sum_{l_f} (M_d + M_e - M_x), \tag{2}$$

where the total energy $E=\epsilon_{nl\lambda}+\epsilon_i=\epsilon_e+\epsilon_f$, $\epsilon=k^2/2$, $S(\lambda)=2(2-\delta_{\lambda,0})$ is the statistical weight of the $nl\lambda$ orbital, and the continuum normalization is chosen as one times a sine function.

The direct scattering term is given by

$$M_d = \sum_{m_i} \sum_{m_e} \sum_{m} \sum_{k} \sum_{k'} \frac{(k-q)\,!\,(k'-q')!}{(k+q)\,!\,(k'+q')!} \times R^{kq*}(\epsilon_f l_f \lambda_f, \epsilon_e l_e \lambda_e; \epsilon_i l_i \lambda_i, nl\lambda) \times R^{k'q'}(\epsilon_f l_f \lambda_f, \epsilon_e l_e \lambda_e; \epsilon_i l_i \lambda_i, nl\lambda), \tag{3}$$

where $q=|m_e-m|\le k$ and $q'=|m_e-m|\le k'$. The exchange scattering term is given by

$$M_e = \sum_{m_i} \sum_{m_e} \sum_{m} \sum_{k} \sum_{k'} \frac{(k-q)\,!\,(k'-q')!}{(k+q)\,!\,(k'+q')!} \times R^{kq*}(\epsilon_e l_e \lambda_e, \epsilon_f l_f \lambda_f; \epsilon_i l_i \lambda_i, nl\lambda) \times R^{k'q'}(\epsilon_e l_e \lambda_e, \epsilon_f l_f \lambda_f; \epsilon_i l_i \lambda_i, nl\lambda), \tag{4}$$

where $q=|m_i-m_e|\le k$ and $q'=|m_i-m_e|\le k'$. The cross scattering term is given by

$$M_x = \sum_{m_i} \sum_{m_e} \sum_{m} \sum_{k} \sum_{k'} \frac{(k-q)\,!\,(k'-q')!}{(k+q)\,!\,(k'+q')!} \times R^{kq*}(\epsilon_f l_f \lambda_f, \epsilon_e l_e \lambda_e; \epsilon_i l_i \lambda_i, nl\lambda) \times R^{k'q'}(\epsilon_e l_e \lambda_e, \epsilon_f l_f \lambda_f; \epsilon_i l_i \lambda_i, nl\lambda), \tag{5}$$

where $q=|m_e-m|\le k$ and $q'=|m_i-m_e|\le k'$.

In all three scattering terms $\lambda_f=|m_i+m-m_e|\le l_f$ and the (r,θ) polar coordinate integral is given by

$$R^{kq}(\epsilon_f l_f \lambda_f, \epsilon_e l_e \lambda_e; \epsilon_i l_i \lambda_i, nl\lambda) = \int_0^\infty dr_1 \int_0^\infty dr_2 \frac{r_<^k}{r_>^{k+1}} \int_0^\pi d\theta_1 \int_0^\pi d\theta_2 P_q^k(\cos\theta_1) P_{q'}^{k'}(\cos\theta_2) \times u^*_{\epsilon_f l_f \lambda_f}(r_1,\theta_1) u^*_{\epsilon_e l_e \lambda_e}(r_2,\theta_2) u_{\epsilon_i l_i \lambda_i}(r_1,\theta_1) u_{nl\lambda}(r_2,\theta_2), \tag{6}$$

where $P_q^k(\cos\theta)=(-1)^q\sqrt{4\pi(k+q)\,!\,/(2k+1)(k-q)!}\,Y_{kq}(\theta,\phi=0)$ are associated Legendre functions, $u_{nl\lambda}(r,\theta)$ are bound reduced orbitals, and $u_{\epsilon l\lambda}(r,\theta)$ are continuum reduced orbitals. The bound and continuum reduced orbitals are defined by

$$\psi(r,\theta,\phi) = \frac{u(r,\theta)}{r\sqrt{\sin\theta}} \frac{e^{im\phi}}{\sqrt{2\pi}}, \tag{7}$$

where $\psi(r,\theta,\phi)$ is the spatial part of the single-particle wave function and the bound normalization is $\int_0^\infty dr \int_0^\pi d\theta [u(r,\theta)]^2 = 1$.

B. Molecular ion potential

The bound orbitals for the molecular ion are calculated using a single-configuration self-consistent-field method based on a linear combination of Slater-type orbitals [14]. The molecular bound orbitals are then transformed [15] onto a two-dimensional (r,θ) numerical lattice to yield bound reduced orbitals $u_{nl\lambda}(r,\theta)$. Using the molecular bound orbitals we construct a Hartree potential with local exchange given by

$$V_{HX}(r,\theta) = V_{direct}(r,\theta) + \alpha V_{exchange}(r,\theta), \tag{8}$$

where α is an adjustable parameter used to achieve the experimental ionization potential for the valence bound orbital of the molecule. The direct potential is given by

$$V_{direct}(r,\theta) = \sum_k V_k(r) P_0^k(\cos\theta), \tag{9}$$

where

$$V_k(r) = \sum_{nl\lambda} w_{nl\lambda} \int_0^\infty dr' \int_0^\pi d\theta' [u_{nl\lambda}(r',\theta')]^2 \frac{r_<^k}{r_>^{k+1}} P_0^k(\cos\theta'). \tag{10}$$

The local exchange potential is given by

$$V_{exchange}(r,\theta) = -\frac{1}{2}\left(\frac{24\rho(r,\theta)}{\pi}\right)^{1/3}, \tag{11}$$

where

$$\rho(r,\theta) = \sum_{nl\lambda} w_{nl\lambda}\frac{[u_{nl\lambda}(r,\theta)]^2}{2\pi r^2 \sin\,\theta}. \tag{12}$$

The sums in Eqs. (10) and (12) are over all bound orbitals for the molecular ion, weighted by their occupation numbers $w_{nl\lambda}$.

C. Molecular wave functions

The bound and continuum orbitals needed to calculate the configuration-average ionization cross section of Eq. (2) are found by solution of the single-particle Schrödinger equation given by

$$\left(-\frac{1}{2}\nabla^2 + V_{nuclear}(r,\theta) + V_{HX}(r,\theta) - \epsilon\right)\psi(r,\theta,\phi) = 0. \tag{13}$$

The nuclear potential is given by

$$V_{nuclear}(r,\theta) = -\frac{Z}{\sqrt{r^2 + \frac{1}{4}R^2 - rR\cos\,\theta}} - \frac{Z}{\sqrt{r^2 + \frac{1}{4}R^2 + rR\cos\,\theta}}, \tag{14}$$

where Z is the charge on each nucleus of a homonuclear diatomic molecule and R is the internuclear separation distance. The variational principle applied to Eq. (13) for a reduced orbital on a two-dimensional (r,θ) numerical lattice yields

$$\begin{aligned} Ku(r_i,\theta_j) &+ [V_{centrifugal}(r_i,\theta_j) + V_{nuclear}(r_i,\theta_j) \\ &+ V_{HX}(r_i,\theta_j) - \epsilon]u(r_i,\theta_j) = 0. \end{aligned} \tag{15}$$

For low-order finite differences with uniform lattice spacings Δr and $\Delta\theta$, the effect of the kinetic energy operator is given by

$$\begin{aligned} Ku(r_i,\theta_j) = &-\frac{1}{2}\left(\frac{c_i u(r_{i+1},\theta_j) + c_{i-1}u(r_{i-1},\theta_j) - \bar{c}_i u(r_i,\theta_j)}{\Delta r^2}\right) \\ &- \frac{1}{2r_i^2}\left(\frac{d_j u(r_i,\theta_{j+1}) + d_{j-1}u(r_i,\theta_{j-1}) - \bar{d}_j u(r_i,\theta_j)}{\Delta\theta^2}\right), \end{aligned} \tag{16}$$

where $c_i = r_{i+1/2}^2/r_i r_{i+1}$, $\bar{c}_i = (r_{i+1/2}^2 + r_{i-1/2}^2)/r_i^2$, $d_j = \sin\,\theta_{j+1/2}/\sqrt{\sin\,\theta_j \sin\,\theta_{j+1}}$, and $\bar{d}_j = (\sin\,\theta_{j+1/2} + \sin\,\theta_{j-1/2})/\sin\,\theta_j$. The centrifugal potential is given by

$$V_{centrifugal}(r,\theta) = \frac{\lambda^2}{2r^2\sin^2\theta}. \tag{17}$$

The valence bound orbital needed to calculate the configuration-average ionization cross section of Eq. (2) is found by matrix diagonalization of the one-electron Hamiltonian found in Eq. (15). For $N_r=3$ and $N_\theta=2$ the Hamiltonian matrix has the block tridiagonal form

$$\mathbf{H} = \begin{pmatrix} T_{11} & D_{11} & C_1 & 0 & 0 & 0 \\ D_{11} & T_{12} & 0 & C_1 & 0 & 0 \\ C_1 & 0 & T_{21} & D_{21} & C_2 & 0 \\ 0 & C_1 & D_{21} & T_{22} & 0 & C_2 \\ 0 & 0 & C_2 & 0 & T_{31} & D_{31} \\ 0 & 0 & 0 & C_2 & D_{31} & T_{32} \end{pmatrix}, \tag{18}$$

where $T_{ij} = \bar{c}_i/2\Delta r^2 + \bar{d}_j/2r_i^2\Delta\theta^2 + V(r_i,\theta_j)$, $D_{ij} = -d_j/2r_i^2\Delta\theta^2$, and $C_i = -c_i/2\Delta r^2$. The parameter α is adjusted in the Hartree potential with local exchange until the matrix diagonalization yields an eigenenergy that agrees with the experimental ionization potential for the valence bound orbital.

The many continuum orbitals needed to calculate the configuration-average ionization cross section of Eq. (2) are found by recasting the one-electron Schrödinger equation of Eq. (15) and the large-r boundary conditions for the continuum orbital as a system of linear equations $\mathbf{Au}=\mathbf{b}$. Following standard WKB theory, we choose S-matrix boundary conditions with long-range unit normalization such that

$$u_{kl\lambda}(r,\theta) = F_{kl\lambda}(r,\theta) + \sum_{l'} S_{ll'}G_{kl'\lambda}(r,\theta), \tag{19}$$

where

$$F_{kl\lambda}(r,\theta) = \sqrt{\frac{k}{4z_l(r)}}e^{i\bar{\phi}_l(r)}\bar{P}_{l\lambda}(\theta), \tag{20}$$

$$G_{kl\lambda}(r,\theta) = \sqrt{\frac{k}{4z_l(r)}}e^{-i\bar{\phi}_l(r)}\bar{P}_{l\lambda}(\theta), \tag{21}$$

$\bar{P}_{l\lambda}(\theta) = \sqrt{2\pi\sin\,\theta}Y_{l\lambda}(\theta,\phi=0)$ is a normalized associated Legendre function, $z_l(r) = d\bar{\phi}_l(r)/dr$, $\bar{\phi}_l(r) = kr + (q/k)\ln 2kr - l\pi/2 + \sigma_l$, $k=\sqrt{2\epsilon}$ is the linear momentum, l is the angular momentum, q is the asymptotic charge, and σ_l is the Coulomb phase shift. For $N_r=3$ and $N_\theta=2$ the continuum linear equations have the block tridiagonal form

$$\begin{pmatrix} T_{11}-\epsilon & D_{11} & C_1 & 0 & 0 & 0 \\ D_{11} & T_{12}-\epsilon & 0 & C_1 & 0 & 0 \\ C_1 & 0 & T_{21}-\epsilon & D_{21} & C_2G_{31}^{l_1} & C_2G_{31}^{l_2} \\ 0 & C_1 & D_{21} & T_{22}-\epsilon & C_2G_{32}^{l_1} & C_2G_{32}^{l_2} \\ 0 & 0 & C_2 & 0 & X_{31}^{l_1} & X_{31}^{l_2} \\ 0 & 0 & 0 & C_2 & X_{32}^{l_1} & X_{32}^{l_2} \end{pmatrix}\begin{pmatrix} u_{11} \\ u_{12} \\ u_{21} \\ u_{22} \\ S_{ll_1} \\ S_{ll_2} \end{pmatrix} = \begin{pmatrix} 0 \\ 0 \\ -C_2F_{31}^{l} \\ -C_2F_{32}^{l} \\ -Y_{31}^{l} \\ -Y_{32}^{l} \end{pmatrix}, \tag{22}$$

where $u_{ij}=u(r_i,\theta_j)$, $F_{ij}^l=F_{kl\lambda}(r_i,\theta_j)$, and $G_{ij}^l=G_{kl\lambda}(r_i,\theta_j)$. The elements of the X and Y matrices are given by $X_{31}^l=(T_{31}-\epsilon)G_{31}^l+C_3G_{41}^l+D_{31}G_{32}^l$, $X_{32}^l=(T_{32}-\epsilon)G_{32}^l+C_3G_{42}^l+D_{31}G_{31}^l$, $Y_{31}^l=(T_{31}-\epsilon)F_{31}^l+C_3F_{41}^l+D_{31}F_{32}^l$, and $Y_{32}^l=(T_{32}-\epsilon)F_{32}^l+C_3F_{42}^l+D_{31}F_{31}^l$. We derive Eq. (22) from Eq. (15), using Eq. (19) for the radial lattice points $i=N_r$ and N_r+1 in the form

$$u_{ij}=F_{ij}^l+S_{ll_1}G_{ij}^{l_1}+S_{ll_2}G_{ij}^{l_2}. \tag{23}$$

We solve for $\mathbf{u}$ by standard LU decomposition of the matrix $\mathbf{A}$. We note that $\mathbf{u}$ contains a discrete representation of the complex continuum orbital $u_{nl\lambda}(r,\theta)$, and elements of the S matrix. A key element in guarding against l mixing in the continuum orbitals is to solve for the normalized associated Legendre functions $\bar{P}_{l\lambda}(\theta)$ by matrix diagonalization of the angular part of the one-electron Hamiltonian found in Eq. (15). For $N_r=N_\theta=2$ the angular Hamiltonian matrix has the tridiagonal form

$$\mathbf{H}_{angular}=\begin{pmatrix} \dfrac{\bar{d}_1}{\Delta\theta^2}+\dfrac{\lambda^2}{\sin^2\theta_1} & -\dfrac{d_1}{\Delta\theta^2} \\ -\dfrac{d_1}{\Delta\theta^2} & \dfrac{\bar{d}_2}{\Delta\theta^2}+\dfrac{\lambda^2}{\sin^2\theta_2} \end{pmatrix}. \tag{24}$$

III. RESULTS

The configuration-average distorted-wave method was used to calculate the electron-impact ionization cross section for H_2 at an internuclear separation of $R=1.4$. We employ a 3000×32 point lattice in (r,θ) spherical polar coordinates with a uniform mesh spacing of $\Delta r=0.1$ and $\Delta\theta=0.03125\pi$. Using a single-configuration self-consistent-field $1s\sigma$ molecular orbital for H_2^+ at $R=1.4$ [14,15], the exchange potential parameter α is adjusted in the diagonalization of Eq. (15) to yield a $1s\sigma$ valence orbital for H_2 with an ionization potential of 15.4 eV. Partial cross sections are calculated for $l_i=0-9$ and $\lambda_i=0-4$ and extrapolated to higher l_i and λ_i using appropriate fitting functions. Total cross sections are calculated at incident energies from $\epsilon_i=20$ to 100 eV and then interpolated over intermediate energies using a B-spline fitting function.

Electron-impact ionization cross section results for H_2 at $R=1.4$ are presented in Fig. 1. The CADW results, shown as the solid line, are about 30% higher than results of an electron beam and gas cell experiment [16] near the peak of the cross section. We note that similar CADW results for the He atom are also about 30% higher than experiment near the peak of the cross section. For comparison, we also present the ionization cross section for H_2 as calculated using a one-parameter binary encounter Bethe (BEB) method, shown as the dashed line. The BEB ionization cross section is given by [17]

$$\sigma_{ion}=4\pi w\left(\frac{I_H}{I_s}\right)^2\left(\frac{\frac{1}{2}\ln(u)\left(1-\frac{1}{u^2}\right)+1-\frac{1}{u}-\frac{\ln(u)}{u+1}}{u+2}\right), \tag{25}$$

where $u=E/I_s$, E is the incident energy, $I_H=13.6$ eV is the ionization potential of atomic hydrogen, and $I_s=15.4$ eV is the ionization potential of molecular hydrogen. The semiempirical binary encounter method has been extensively generalized to accurately predict total ionization cross sections for many atoms and molecules and their ions [18]. We also note that recent *ab initio* nonperturbative R-matrix-with-pseudostates [5] and time-dependent close-coupling [6] calculations of total cross sections for the electron-impact ionization of H_2 are in excellent agreement with experiment.

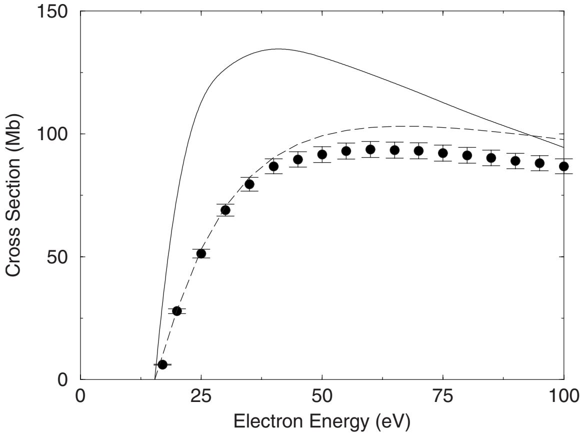

FIG. 1. Electron-impact ionization of H_2. Solid curve, configuration-average distorted-wave method; dashed curve, binary encounter Bethe method; solid circles, experiment [16] ($1\ \text{Mb}=10^{-18}\ \text{cm}^2$).

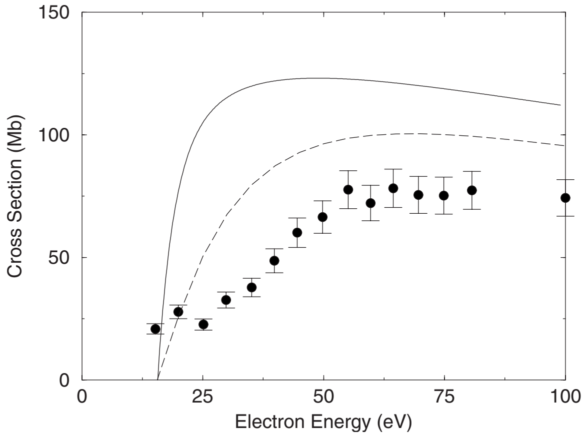

FIG. 2. Electron-impact ionization of N_2. Solid curve, configuration-average distorted-wave method; dashed curve, binary encounter Bethe method; solid circles, experiment [19] (1 Mb $=10^{-18}$ cm^2).

The configuration-average distorted-wave method was used to calculate the electron-impact ionization cross section for $N_2(^1\Sigma_g^+) \rightarrow N_2{}^+(^2\Sigma_g^+)$ at an internuclear separation of $R=2.1$. We employ a $15{,}000 \times 32$ point lattice in (r,θ) spherical polar coordinates with a uniform mesh spacing of $\Delta r=0.02$ and $\Delta\theta=0.03125\pi$. Using single-configuration self-consistent-field $1s\sigma$, $2s\sigma$, $2p\sigma$, $2p\pi$, $3s\sigma$, and $3p\sigma$ molecular orbitals for $N_2{}^+$ at $R=2.1$ [14,15], the exchange potential parameter α is adjusted in the diagonalization of Eq. (15) to yield a $3s\sigma$ valence orbital for N_2 with an ionization potential of 15.7 eV. Partial cross sections are calculated for $l_i=0-10$ and $\lambda_i=0-6$, and extrapolated to higher l_i and λ_i using appropriate fitting functions. Total cross sections are calculated at incident energies from $\epsilon_i=20$ to 100 eV and then interpolated over intermediate energies using a three-parameter fitting function.

Electron-impact ionization cross section results for N_2 at $R=2.1$ are presented in Fig. 2. The CADW results, shown as the solid line, are about 50% higher than an electron beam, gas cell, and laser-induced fluorescence experiment [19] near the peak of the cross section. We note that similar CADW results for the Si atom are also about 50% higher than experiment near the peak of the cross section. For comparison we also present BEB results with $I_s=15.7$ eV, shown as the dashed line.

IV. SUMMARY

In conclusion, we have applied a configuration-average distorted-wave method to calculate electron-impact ionization cross sections for H_2 and N_2. A single-configuration self-consistent-field method was used to generate the molecular orbitals for H_2^+ and N_2^+ needed to construct a Hartree potential with local exchange. Valence bound orbitals for H_2 and N_2 were obtained by matrix diagonalization of the single-particle Schrödinger equation. Distorted-wave continuum orbitals were obtained using a new algorithm to solve the 2D radial and angular Schrödinger equation. The key modification is the inclusion of the full S matrix in the standard LU decomposition numerical method. Total distorted-wave cross section results for H_2 and N_2 are found to be between 30% and 50% higher than recent experimental measurements, in keeping with the usual range of accuracy found for distorted-wave calculations of the electron ionization of ground-state neutral atoms.

In the future, we plan to apply the molecular CADW method to calculate electron-impact excitation and ionization processes in a wide variety of diatomic molecules and their ions. Although the number of radial grid points needed to adequately describe the heavier diatomic molecules, like N_2, may be significantly reduced by employing a variable mesh spacing, the overall accuracy of a first-order perturbative method remains limited. On the other hand, the further development and application of nonperturbative approaches, like the R-matrix-with-pseudostates and time-dependent close-coupling methods, will improve the accuracy of truly *ab initio* predictions of electron ionization cross sections for molecules. In addition, the new CADW method for solving the 2D radial and angular Schrödinger equation for continuum distorted-waves is being used with great success to produce projection states to extract energy and angle differential cross sections in nonperturbative time-dependent close-coupling calculations for the double photoionization of H_2 [20] and the electron single ionization of H_2 and other diatomic molecules.

ACKNOWLEDGMENTS

This work was supported in part by grants from the U.S. Department of Energy. Computational work was carried out at the National Energy Research Scientific Computing Center in Oakland, California and at the National Center for Computational Sciences in Oak Ridge, Tennessee.

---

[1] *Nuclear Fusion Research*, edited by R. E. H. Clark and D. H. Reiter, Chemical Physics Series Vol. 78 (Springer, Berlin, 2005).
[2] A. J. Murray, J. Phys. B **38**, 1999 (2005).
[3] D. S. Milne-Brownlie, M. Foster, J. Gao, B. Lohmann, and D. H. Madison, Phys. Rev. Lett. **96**, 233201 (2006).
[4] M. S. Pindzola, F. Robicheaux, and J. Colgan, J. Phys. B **38**, L285 (2005).
[5] J. D. Gorfinkiel and J. Tennyson, J. Phys. B **38**, 1607 (2005).
[6] M. S. Pindzola, F. Robicheaux, S. D. Loch, and J. P. Colgan, Phys. Rev. A **73**, 052706 (2006).
[7] J. C. Tully and R. S. Berry, J. Chem. Phys. **51**, 2056 (1969).
[8] J. A. Richards and F. P. Larkins, J. Phys. B **17**, 1015 (1984); **19**, 1945 (1986).
[9] C. A. Weatherford, M. Dong, and B. C. Saha, Int. J. Quantum Chem. **65**, 591 (1997).

[10] M. S. Pindzola, D. C. Griffin, and C. Bottcher, in *Atomic Processes in Electron-Ion and Ion-Ion Collisions*, edited by F. Brouillard, NATO Advanced Studies Institute, Series B: Physics (Plenum Press, New York, 1986), Vol. 145, p. 75.

[11] M. S. Pindzola, F. Robicheaux, J. A. Ludlow, J. Colgan, and D. C. Griffin, Phys. Rev. A **72**, 012716 (2005).

[12] F. Robicheaux, J. Phys. B **29**, 779 (1996).

[13] M. S. Pindzola and F. J. Robicheaux, Phys. Rev. A **61**, 052707 (2000).

[14] Theoretical Chemistry Group, Computer code ALCHEMY (IBM Research Laboratory, San Jose, CA, 1970).

[15] M. A. Morrison, Comput. Phys. Commun. **21**, 63 (1980).

[16] H. C. Straub, P. Renault, B. G. Lindsay, K. A. Smith, and R. F. Stebbings, Phys. Rev. A **54**, 2146 (1996).

[17] Y. K. Kim and M. E. Rudd, Phys. Rev. A **50**, 3954 (1994).

[18] W. M. Huo, Phys. Rev. A **64**, 042719 (2001).

[19] N. Abramzon, R. B. Siegel, and K. Becker, J. Phys. B **32**, L247 (1999).

[20] J. Colgan, M. S. Pindzola, and F. Robicheaux, Phys. Rev. Lett. **98**, 153001 (2007).